Analytical study of optical bistability in silicon-waveguide resonators

Ivan D. Rukhlenko,[1,*] **Malin Premaratne,**[1] **and Govind P. Agrawal**[2]

[1]*Advanced Computing and Simulation Laboratory (AχL)*
Department of Electrical and Computer Systems Engineering
Monash University, Melbourne, VIC 3800, Australia
[2]*Institute of Optics, University of Rochester, Rochester, NY 14627, USA*
ivan.rukhlenko@eng.monash.edu.au

Abstract: We present a theoretical model that describes accurately the nonlinear phenomenon of optical bistability in silicon-waveguide resonators but remains amenable to analytical results. Using this model, we derive a transcendental equation governing the intensity of a continuous wave transmitted through a Fabry–Perot resonator formed using a silicon-on-insulator waveguide. This equation reveals a dual role of free carriers in the formation of optical bistability in silicon. First, it shows that free-carrier absorption results in a saturation of the transmitted intensity. Second, the free-carrier dispersion and the thermo-optic effect may introduce phase shifts far exceeding those resulting from the Kerr effect alone, thus enabling one to achieve optical bistability in ultrashort resonators that are only a few micrometers long. Bistability can occur even when waveguide facets are not coated because natural reflectivity of the silicon–air interface can provide sufficient feedback. We find that it is possible to control the input-output characteristics of silicon-based resonators by changing the free-carrier lifetime using a reverse-biased p-n junction. We show theoretically that such a technique is suitable for realization of electronically assisted optical switching at a fixed input power and it may lead to silicon-based, nanometer-size, optical memories.

OCIS codes: (190.1450) Bistability; (040.6040) Silicon; (250.4390) Nonlinear optics, integrated optics; (230.4320) Nonlinear optical devices; (140.4780) Optical resonators; (250.6715) Switching; (160.6840) Thermo-optical materials; (230.7370) Waveguides.

References and links

1. B. Jalali, S. Yegnanarayanan, T. Yoon, T. Yoshimoto, I. Rendina, and F. Coppinger, "Advances in silicon-on-insulator optoelectronics," IEEE J. Sel. Top. Quantum Electron. **4**, 938–947 (1998).
2. G. T. Reed and A. P. Knights, *Silicon Photonics: An Introduction* (Wiley, Hoboken, 2004).
3. O. Boyraz, P. Koonath, V. Raghunathan, and B. Jalali, "All optical switching and continuum generation in silicon waveguides," Opt. Express **12**, 4094–4102 (2004).
4. B. Jalali, O. Boyraz, V. Raghunathan, D. Dimitropoulos, and P. Koonath, "Silicon Raman amplifiers, lasers and their applications," in *Active and Passive Optical Components for WDM Communications V*, A. K. Dutta, Y. Ohishi, N. K. Dutta, and J. Moerk, Eds., Proc. SPIE **6014**, 21–26 (2005).
5. R. A. Soref, "The past, present, and future of silicon photonics," IEEE J. Sel. Top. Quantum Electron. **12**, 1678–1687 (2006).
6. B. Jalali, V. Raghunathan, D. Dimitropoulos, and O. Boyraz, "Raman-based silicon photonics," IEEE J. Sel. Top. Quantum Electron. **12**, 412–421 (2006).
7. M. Dinu, F. Quochi, and H. Garcia, "Third-order nonlinearities in silicon at telecom wavelengths," Appl. Phys. Lett. **82**, 2954–2956 (2003).

#118020 - $15.00 USD Received 1 Oct 2009; revised 6 Nov 2009; accepted 17 Nov 2009; published 18 Nov 2009

8. R. S. Jacobsen, K. N. Andersen, P. I. Borel, J. Fage-Pedersen, L. H. Frandsen, O. Hansen, M. Kristensen, A. V. Lavrinenko, G. Moulin, H. Ou, C. Peucheret, B. Zsigri, and A. Bjarklev, "Strained silicon as a new electro-optic material," Nature **441**, 199–202 (2006).
9. H. K. Tsang and Y. Liu, "Nonlinear optical properties of silicon waveguides," Semicond. Sci. Technol. **23**, 064007(1–9) (2008).
10. R. Claps, D. Dimitropoulos, and B. Jalali, "Stimulated Raman scattering in silicon waveguides," Electron. Lett. **38**, 1352–1354 (2002).
11. R. Claps, D. Dimitropoulos, V. Raghunathan, Y. Han, and B. Jalali, "Observation of stimulated Raman amplification in silicon waveguides," Opt. Express **11**, 1731–1739 (2003).
12. T. K. Liang and H. K. Tsang, "Role of free carriers from two-photon absorption in Raman amplification in silicon-on-insulator waveguides," Appl. Phys. Lett. **84**, 2745–2747 (2004).
13. R. Claps, V. Raghunathan, D. Dimitropoulos, and B. Jalali, "Influence of nonlinear absorption on Raman amplification in silicon-on-insulator waveguides," Opt. Express **12**, 2774–2780 (2004).
14. O. Boyraz and B. Jalali, "Demonstration of 11 dB fiber-to-fiber gain in a silicon Raman amplifier," IEICE Electron. Exp. **1**, 429–434 (2004).
15. A. Liu, H. Rong, M. Paniccia, O. Cohen, and D. Hak, "Net optical gain in a low loss silicon-on-insulator waveguide by stimulated Raman scattering," Opt. Express **12**, 4261–4268 (2004).
16. R. Espinola, J. Dadap, R. Osgood, S. J. McNab, and Y. A. Vlasov, "Raman amplification in ultrasmall silicon-on-insulator wire waveguides," Opt. Express **12**, 3713–3718 (2004).
17. R. Jones, H. Rong, A. Liu, A. W. Fang, M. J. Paniccia, D. Hak, and O. Cohen, "Net continuous-wave optical gain in a low loss silicon-on-insulator waveguide by stimulated Raman scattering," Opt. Express **13**, 519–525 (2005).
18. S. Fathpour, K. K. Tsia, and B. Jalali, "Energy harvesting in silicon Raman amplifiers," Appl. Phys. Lett. **89**, 061109(1–3) (2006).
19. R. Jones, A. Liu, H. Rong, M. Paniccia, O. Cohen, and D. Hak, "Lossless optical modulation in a silicon waveguide using stimulated Raman scattering," Opt. Express **13**, 1716–1723 (2005).
20. R. Claps, D. Dimitropoulos, Y. Han, and B. Jalali, "Observation of Raman emission in silicon waveguides at 1.54 μm," Opt. Express **10**, 1305–1313 (2002).
21. M. Krause, H. Renner, and E. Brinkmeyer, "Analysis of Raman lasing characteristics in silicon-on-insulator waveguides," Opt. Express **12**, 5703–5710 (2004).
22. O. Boyraz and B. Jalali, "Demonstration of a silicon Raman laser," Opt. Express **12**, 5269–5273 (2004).
23. H. Renner, M. Krause, and E. Brinkmeyer, "Maximal gain and optimal taper design for Raman amplifiers in silicon-on-insulator waveguides," in *Integrated Photonics Research and Applications Topical Meetings* (IPRA 2005), paper JWA3.
24. H. Rong, A. Liu, R. Jones, O. Cohen, D. Hak, R. Nicolaescu, A. Fang, and M. Paniccia, "An all-silicon Raman laser," Nature **433**, 292–294 (2005).
25. M. Krause, H. Renner, and E. Brinkmeyer, "Efficiency increase of silicon-on-insulator Raman lasers by reduction of free-carrier absorption in tapered waveguides," in *Conference on Lasers and Electro-Optics* (CLEO 2005), paper CThB1.
26. H. Rong, R. Jones, A. Liu, O. Cohen, D. Hak, A. Fang, and M. Pannicia, "A continuous-wave Raman silicon laser," Nature **433**, 725–728 (2005).
27. O. Boyraz and B. Jalali, "Demonstration of directly modulated silicon Raman laser," Opt. Express **13**, 796–800 (2005).
28. M. Krause, H. Renner, and E. Brinkmeyer, "Efficient Raman lasing in tapered silicon waveguides," Spectroscopy **21**, 26–32 (2006).
29. J. Zhang, Q. Lin, G. Piredd, R. W. Boyd, G. P. Agrawal, and P. M. Fauchet, "Optical solitons in a silicon waveguide," Opt. Express **15**, 7682–7688 (2007).
30. O. Boyraz, T. Indukuri, and B. Jalali, "Self-phase-modulation induced spectral broadening in silicon waveguides," Opt. Express **12**, 829–834 (2004).
31. L. Yin, Q. Lin, and G. P. Agrawal, "Soliton fission and supercontinuum generation in silicon waveguides," Opt. Lett. **32**, 391–393 (2007).
32. I-W. Hsieh, X. Chen, X. Liu, J. I. Dadap, N. C. Panoiu, C. Y. Chou, F. Xia, W. M. Green, Y. A. Vlasov, and R. M. Osgood, Jr., "Supercontinuum generation in silicon photonic wires," Opt. Express **15**, 15242–15249 (2007).
33. R. Dekker, A. Driessen, T. Wahlbrink, C. Moormann, J. Niehusmann, and M. Först, "Ultrafast Kerr-induced all-optical wavelength conversion in silicon waveguides using 1.55 μm femtosecond pulses," Opt. Express **14**, 8336–8346 (2006).
34. E. Dulkeith, Y. A. Vlasov, X. Chen, N. C. Panoiu, and R. M. Osgood, Jr., "Self-phase-modulation in submicron silicon-on-insulator photonic wires," Opt. Express **14**, 5524–5534 (2006).
35. D. J. Moss, L. Fu, I. Littler, and B. J. Eggleton, "Ultrafast all-optical modulation via two-photon absorption in silicon-on-insulator waveguides," IEEE Electron. Lett. **41**, 320–321 (2005).
36. M. W. Geis, S. J. Spector, R. C. Williamson, and T. M. Lyszczarz, "Submicrosecond, submilliwatt, silicon-on-insulator thermooptic switch," IEEE Photon. Technol. Lett. **16**, 2514–2516 (2004).
37. T. K. Liang, L. R. Nunes, M. Tsuchiya, K. S. Abedin, T. Miyazaki, D. V. Thourhout, W. Bogaerts, P. Dumon, R.

#118020 - $15.00 USD Received 1 Oct 2009; revised 6 Nov 2009; accepted 17 Nov 2009; published 18 Nov 2009

Baets, and H. Tsang, "High speed logic gate using two-photon absorption in silicon waveguides," Opt. Commun. **265**, 171–174 (2006).
38. H. K. Tsang, C. S. Wong, T. K. Liang, I. E. Day, S. W. Roberts, A. Harpin, J. Drake, and M. Asghari, "Optical dispersion, two-photon absorption, and self-phase modulation in silicon waveguides at 1.5 μm wavelength," Appl. Phys. Lett. **80**, 416–418 (2002).
39. T. Liang, L. Nunes, T. Sakamoto, K. Sasagawa, T. Kawanishi, M. Tsuchiya, G. Priem, D. V. Thourhout, P. Dumon, R. Baets, and H. Tsang, "Ultrafast all-optical switching by cross-absorption modulation in silicon wire waveguides," Opt. Express **13**, 7298–7303 (2005).
40. E. K. Tien, N. S. Yuksek, F. Qian, and O. Boyraz, "Pulse compression and modelocking by using TPA in silicon waveguides," Opt. Express **15**, 6500–6506 (2007).
41. E. K. Tien, F. Qian, N. S. Yuksek, and O. Boyraz, "Influence of nonlinear loss competition on pulse compression and nonlinear optics in silicon," Appl. Phys. Lett. **91**, 201115(1–3) (2007).
42. D. Dimitropoulos, B. Houshmand, R. Claps, and B. Jalali, "Coupled-mode theory of Raman effect in silicon-on-insulator waveguides," Opt. Lett. **28**, 1954–1956 (2003).
43. V. M. N. Passaro and F. D. Leonardis, "Space-time modeling of Raman pulses in silicon-on-insulator optical waveguides," J. Lightwave Technol. **24**, 2920–2931 (2006).
44. X. Chen, N. C. Panoiu, and R. M. Osgood, "Theory of Raman-mediated pulsed amplification in silicon-wire waveguides," IEEE J. Quantum Electron. **42**, 160–170 (2006).
45. Q. Lin, O. J. Painter, and G. P. Agrawal, "Nonlinear optical phenomena in silicon waveguides: Modeling and applications," Opt. Express **15**, 16604–16644 (2007).
46. L. Yin, Q. Lin, and G. P. Agrawal, "Dispersion tailoring and soliton propagation in silicon waveguides," Opt. Lett. **31**, 1295–1297 (2006).
47. L. Yin and G. P. Agrawal, "Impact of two-photon absorption on self-phase modulation in silicon waveguides," Opt. Lett. **31**, 1295–1297 (2006).
48. V. M. N. Passaro and F. D. Leonardis, "Solitons in SOI optical waveguides," Adv. Studies Theor. Phys. **2**, 769–785 (2008).
49. C. Dissanayake, I. D. Rukhlenko, M. Premaratne, and G. P. Agrawal, "Raman-mediated nonlinear interactions in silicon waveguides: Copropagating and counterpropagating pulses," IEEE Photon. Technol. Lett. **21**, 1372–1374 (2009).
50. I. D. Rukhlenko, M. Premaratne, C. Dissanayake, and G. P. Agrawal, "Nonlinear pulse evolution in silicon waveguides: An approximate analytic approach," J. Lightwave Technol. **27**, 3241–3248 (2009).
51. I. D. Rukhlenko, M. Premaratne, C. Dissanayake, and G. P. Agrawal, "Continuous-wave Raman amplification in silicon waveguides: Beyond the undepleted pump approximation," Opt. Lett. **34**, 536–538 (2009).
52. I. D. Rukhlenko, M. Premaratne, and G. P. Agrawal, "Nonlinear silicon photonics: Analytical tools," IEEE J. Sel. Top. Quantum Electron., in press.
53. I. D. Rukhlenko, C. Dissanayake, M. Premaratne, and G. P. Agrawal, "Maximization of net optical gain in silicon-waveguide Raman amplifiers," Opt. Express **17**, 5807–5814 (2009).
54. I. D. Rukhlenko, C. Dissanayake, M. Premaratne, and G. P. Agrawal, "Optimization of Raman amplification in silicon waveguides with finite facet reflectivities," IEEE J. Sel. Top. Quantum Electron., in press.
55. S. Roy, S. K. Bhadra, and G. P. Agrawal, "Femtosecond pulse propagation in silicon waveguides: Variational approach and its advantages," Opt. Commun. **281**, 5889–5893 (2008).
56. S. Roy, S. K. Bhadra, and G. P. Agrawal, "Raman amplification of optical pulses in silicon waveguides: effects of finite gain bandwidth, pulse width, and chirp," J. Opt. Soc. Am. B **26**, 17–25 (2009).
57. R. Claps, D. Dimitropoulos, V. Raghunathan, Y. Han, and B. Jalali, "Observation of stimulated Raman scattering in silicon waveguides," Opt. Express **11**, 1731–1739 (2003).
58. T. K. Liang and H. K. Tsang, "Nonlinear absorption and Raman scattering in silicon-on-insulator optical waveguides," IEEE J. Sel. Top. Quantum Electron. **10**, 1149–1153 (2004).
59. A. R. Cowan, G. W. Rieger, and J. F. Young, "Nonlinear transmission of 1.5 μm pulses through single-mode silicon-on-insulator waveguide structures," Opt. Express **12**, 1611–1621 (2004).
60. G. W. Rieger, K. S. Virk, and J. F. Yong, "Nonlinear propagation of ultrafast 1.5 μm pulses in high-index-contrast silicon-on-insulator waveguides," Appl. Phys. Lett. **84**, 900–902 (2004).
61. D. Dimitripoulos, R. Jhavery, R. Claps, J. C. S. Woo, and B. Jalali, "Lifetime of photogenerated carriers in silicon-on-insulator rib waveguides," Appl. Phys. Lett. **86**, 071115(1–3) (2005).
62. A. C. Turner, C. Manolatou, B. S. Schmidt, M. Lipson, M. A. Foster, J. E. Sharping, and A. L. Gaeta, "Tailored anomalous GVD in Si channel waveguides," Opt. Express **14**, 4357–4362 (2006).
63. I-W. Hsieh, X. Chen, J. I. Dadap, N. C. Panoiu, and R. M. Osgood, Jr., "Cross-phase modulation-induced spectral and temporal effects on co-propagating femtosecond pulses in silicon photonic wires," Opt. Express **15**, 1135–1146 (2007).
64. I-W. Hsieh, X. Chen, J. I. Dadap, N. C. Panoiu, R. M. Osgood, Jr., S. J. McNab, and Y. A. Vlasov, "Ultrafast-pulse self-phase modulation and third-order dispersion in Si photonic wire-waveguides," Opt. Express **14**, 12380–12387 (2006).
65. E. Dulkeith, F. Xia, L. Schares, W. M. J. Green, and Y. A. Vlasov, "Group index and group velocity dispersion

#118020 - $15.00 USD Received 1 Oct 2009; revised 6 Nov 2009; accepted 17 Nov 2009; published 18 Nov 2009

in silicon on insulator photonic wires," Opt. Express **14**, 3853–3863 (2006).
66. H. J. Eichler, T. Brand, M. Glotz, and B. Smandek, "Optical nonlinearity and bistability in silicon," Phys. Stat. Sol. (b) **150**, 705–718 (1988).
67. V. R. Almeida and M. Lipson, "Optical bistability on a silicon chip," Opt. Lett. **29**, 2387–2389 (2004).
68. G. Priem, P. Dumon, W. Bogaerts, D. V. Thourhout, G. Morthier, and R. Baets, "Optical bistability and pulsating behaviour in silicon-on-insulator ring resonator structures," Opt. Express **13**, 9623–9628 (2005).
69. Q. Xu and M. Lipson, "Carrier-induced optical bistability in silicon ring resonators," Opt. Lett. **31**, 341–343 (2006).
70. Q. Xu and M. Lipson, "All-optical logic based on silicon micro-ring resonators," Opt. Express **15**, 924–929 (2007).
71. G. P. Agrawal, *Applications of Nonliner Fiber Optics*, 2nd ed. (Academic Press, Boston, 2008).
72. R. W. Boyd, *Nonlinear Optics*, (Academic, Boston, 2003).
73. G. P. Agrawal, *Nonlinear Fiber Optics*, 4th ed. (Academic, Boston, 2007).

1. Introduction

Silicon and silicon-on-insulator (SOI) technology are considered to be promising candidates for future optical integration because they enable one to tightly confine and manipulate light in optical devices of subwavelength dimensions. The variety of physical phenomena occurring in silicon near the telecommunication wavelength of 1.55 μm makes it a perfect material for a multitude of photonic devices [1–6]. Among the important nonlinear phenomena that have already been observed in SOI waveguides are: stimulated Raman scattering (SRS) [7–9] used for making optical amplifiers [10–18], modulators [19], and lasers [20–28]; the Kerr effect that has been used for soliton formation [29], supercontinuum generation [3, 30–32], and optical phase modulation [33, 34]; two-photon absorption (TPA) that has been used for optical phase modulation [35]; thermo-optic effect that is suitable for all-optical switching [36, 37]; free-carrier absorption (FCA) and free-carrier dispersion (FCD) that have been employed for all-optical switching [38, 39], and pulse compression [40, 41]. Often, several of these phenomena manifest simultaneously in silicon and thus hinder the possibility of a full analytical description of wave propagation in SOI waveguides.

Owing to the immense practical applications of silicon, a considerable body of research has been done recently to address the problem of light propagation through SOI waveguides. Particularly, an exhaustive theory of nonlinear optical phenomena in SOI waveguides has been presented in Refs. [42–45]. Based on this theory, a number of numerical [21, 23, 25, 28, 29, 46–49], analytical [50–52], and semi-analytical works [53–56], analyzing different aspects of light-matter interaction in silicon waveguides, have been carried out by several research groups. The results of these studies are in excellent agreement with experimental data [57–65] and they validate the underlined theoretical formalism.

An important problem associated with light propagation through silicon that has not been addressed theoretically so far is the nonlinear phenomenon of optical bistability [66]. This effect has been demonstrated experimentally by several research groups using a ring resonator coupled laterally to a single waveguide [67–70]. Even though the reported experimental results were accompanied by comprehensive physical explanations, a unified analytical theory of optical bistability in silicon waveguides is not yet available. In this paper, for the first time to the best of our knowledge, we theoretically analyze the problem of optical bistability in SOI-waveguide resonators of the Fabry–Perot type operating in the continuous-wave (CW) regime. We start from general equations describing evolution of the electric fields associated with the forward- and backward-propagating optical modes that are excited by a light beam launched into a SOI waveguide. We solve these equations analytically and use the obtained solution to calculate the resonator transmittance function in the absence of thermo-optic effect. After that, we modify the transmittance function to the case where thermo-optic effect is not negligible, analyze it analytically, and provide numerical examples supporting our conclusions. Finally, we

#118020 - $15.00 USD Received 1 Oct 2009; revised 6 Nov 2009; accepted 17 Nov 2009; published 18 Nov 2009

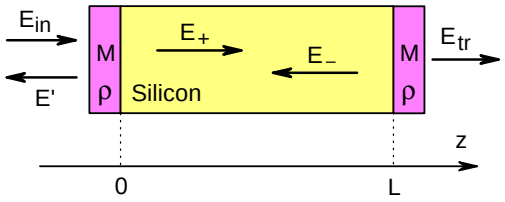

Fig. 1. Schematic of a Fabry–Perot resonator formed by a silicon waveguide of length L and two mirrors (M) with reflectivity ρ^2. The notations used for various electric field amplitudes are also indicated.

propose a new switching scheme utilizing the dependance of the resonator transmittance on the free-carrier lifetime. This scheme is suitable for all-optical switching with fixed bias intensity.

2. Analytical model of optical bistability in silicon resonators

2.1. Propagation equations

Let us consider a Fabry–Perot resonator [71] formed by a SOI waveguide of length L placed between two mirrors with reflectivity ρ^2 (see Fig. 1). The electric field of a CW optical beam in such a waveguide is the sum of the forward- and the backward-propagating waves,

$$E(\mathbf{r},t) = F(x,y)[E_+(z)+E_-(z)]\exp(-i\omega t)+\text{c.c.},$$

where $F(x,y)$ is the lateral profile of the propagating mode and ω is the optical frequency. The functions $E_\pm(z)$, describing evolution of the optical field along the waveguide, can be expressed in the terms of amplitudes $A_\pm(z)$ (representing the square root of corresponding intensities) as follows:

$$E_\pm(z) = \varpi A_\pm(z)\exp(\pm i\beta_0 z),$$

where $\varpi = (\mu_0/\varepsilon_0)^{1/4}(2n_0)^{-1/2}$ is the mapping factor, μ_0 and ε_0 are, respectively, the intrinsic permeability and permittivity of vacuum, n_0 is the linear refractive index, $\beta_0 = n_0 k$ is the propagation constant, $k = \omega/c$, and c is the speed of light in vacuum. The amplitudes $A_\pm(z)$ are known to satisfy the following evolution equations [44, 45]:

$$\pm\frac{1}{A_\pm}\frac{\mathrm{d}A_\pm}{\mathrm{d}z} = -\frac{\alpha}{2}+i\gamma(1+ir)\left(|A_\pm|^2+2|A_\mp|^2\right)-\frac{\sigma}{2}(1+i\mu)N, \tag{1}$$

where α describes linear losses, $\gamma = kn_2$ accounts for the Kerr effect characterized by the nonlinear parameter n_2, and $r = \beta/(2\gamma)$ represents the effect of TPA governed by the coefficient β. The free-carrier effects are described by the last term in Eqs. (1), where the free-carrier density in the CW case is given by [45]

$$N(z) = \frac{\tau\beta}{2\hbar\omega}\left(|A_\pm|^4+|A_\mp|^4+4|A_\pm A_\mp|^2\right), \tag{2}$$

and it depends on the effective free-carrier lifetime τ. The FCA and FCD effects also depend on the parameters $\sigma = \sigma_r(k_r/k)^2$ and $\mu = 2k\sigma_n/\sigma_r$, where $\sigma_r = 1.45\times10^{-21}$ m^2, $2\pi/k_r = 1.55\,\mu$m, and $\sigma_n = 5.3\times10^{-27}$ m^3 [45].

An important assumption, implicit in the derivation of Eqs. (1), is that the linear refractive index remains constant in the presence of nonlinear processes inside the resonator. Generally, that is not the case since both the TPA and free-carrier recombination may lead to elevation of

#118020 - $15.00 USD Received 1 Oct 2009; revised 6 Nov 2009; accepted 17 Nov 2009; published 18 Nov 2009

local temperature and a corresponding increase in the linear refractive index. To keep n_0 constant, one needs to effectively extract the heat from the waveguide and maintain its temperature fixed. It may also be possible to eliminate the dependance of refractive index on temperature by introducing strain into the SOI waveguide during the fabrication process because any strain reduces the thermo-optic coefficient in silicon [8, 69]. In what follows, we first consider the simpler case where the thermo-optic effect is absent and take it into account in the subsequent analysis.

2.2. Analytical solution of the propagation equations

To find the intensity transmitted through the SOI-waveguide resonator, we need to solve Eqs. (1) together with the appropriate boundary conditions. For this purpose, we introduce four real variables according to the equation

$$A_{\pm}(z) = \sqrt{I_{\pm}(z)}\,\exp[i\phi_{\pm}(z)].$$

Here, $I_{\pm}(z)$ are the intensities of the forward- and backward-propagating modes, that are related to the corresponding powers $P_{\pm}(z)$ through an effective mode area A_{eff} as $I_{\pm}(z) = P_{\pm}(z)/A_{\text{eff}}$. Using Eq. (2), Eqs. (1) can be rewritten in terms of the new variables as

$$\pm\frac{1}{I_{\pm}}\frac{\mathrm{d}I_{\pm}}{\mathrm{d}z} = -\alpha - \beta\,(I_{\pm}+2I_{\mp}) - \xi_r\big(I_+^2+I_-^2+4I_+I_-\big), \tag{3a}$$

$$\pm\frac{\mathrm{d}\phi_{\pm}}{\mathrm{d}z} = \gamma(I_{\pm}+2I_{\mp}) - \xi_i\big(I_+^2+I_-^2+4I_+I_-\big), \tag{3b}$$

where $\xi_r = \sigma\tau\beta/(2\hbar\omega)$ and $\xi_i = \sigma\mu\tau\beta/(4\hbar\omega)$. Unfortunately, Eqs. (3) do not allow a closed-form solution, and we need to make some approximations to proceed further.

As we have shown previously [51], one can ignore the impact of TPA on the intensity of a single CW wave propagating through a silicon waveguide. The same holds for two CW waves if the linear-loss coefficient and the effective free-carrier lifetime are not very small and satisfy the relation $\alpha\xi_r \gg \beta^2$. This condition is readily obtained by comparing the TPA terms with the linear-loss and FCA terms in Eqs. (3a). It is usually satisfied in practice (e.g., for $\alpha \gtrsim 1$ dB/cm and $\tau \gtrsim 1$ ns), and we assume this to be the case in the following analysis.

If we discard the TPA terms in Eqs. (3a), they can be solved analytically by following the method discussed in Ref. [52]. The final result is given by

$$I_+(z) = \sqrt{a\coth(qz+C_2)-b}, \quad I_-(z) = \frac{C_1}{I_+(z)}, \tag{4}$$

where C_1 and C_2 are the integration constants and

$$a = \frac{q}{2\xi_r}, \quad b = 2C_1 + \frac{\alpha}{2\xi_r}, \quad q = \sqrt{(\alpha+2\xi_rC_1)(\alpha+6\xi_rC_1)}.$$

Using this solution in Eqs. (3b) and integrating them, we obtain

$$\phi_+(z) = C_3 + \gamma[\mathscr{J}_1(z) + 2\,\mathscr{J}_2(z)] - \xi_i\,\mathscr{J}_3(z), \tag{5a}$$

$$\phi_-(z) = C_4 - \gamma[\mathscr{J}_2(z) + 2\,\mathscr{J}_1(z)] + \xi_i\,\mathscr{J}_3(z), \tag{5b}$$

#118020 - $15.00 USD Received 1 Oct 2009; revised 6 Nov 2009; accepted 17 Nov 2009; published 18 Nov 2009

where C_3 and C_4 are the integration constants and

$$\mathscr{J}_1(z) = \frac{1}{q}\left\{\sqrt{b-a}\tan^{-1}\left[\frac{I_+(z)}{\sqrt{b-a}}\right] - \sqrt{b+a}\tan^{-1}\left[\frac{I_+(z)}{\sqrt{b+a}}\right]\right\}, \tag{6a}$$

$$\mathscr{J}_2(z) = \frac{C_1}{q}\left\{\frac{1}{\sqrt{b+a}}\tan^{-1}\left[\frac{I_+(z)}{\sqrt{b+a}}\right] - \frac{1}{\sqrt{b-a}}\tan^{-1}\left[\frac{I_+(z)}{\sqrt{b-a}}\right]\right\}, \tag{6b}$$

$$\mathscr{J}_3(z) = \frac{C_1}{2q}\left\{\frac{4(b+a)-C_1}{b+a}\ln G_+(z) - \frac{4(b-a)-C_1}{b-a}\ln G_-(z)\right\} + \frac{a}{q}\ln[\sinh(qz+C_2)] - \frac{2a}{q}\frac{C_1^2}{b^2-a^2}\ln I_+(z) - bz, \tag{6c}$$

with $G_\pm(z) = \coth(qz+C_2)\pm 1$. It is worth noting that, even though we can discard TPA terms in Eqs. (3a), the omission of similar Kerr terms in Eqs. (3b) is not possible since it will lead to high inaccuracy in phase at low input intensities.

The four integration constants C_j ($j = 1,2,3,4$) are determined by using the boundary conditions at resonator facets $z = 0$ and $z = L$,

$$E_+(0) = (1-\rho^2)^{1/2}E_{\text{in}} + \rho E_-(0), \tag{7a}$$

$$E_-(L) = \rho E_+(L). \tag{7b}$$

These two conditions constitute a set of four real equations that allow us to determine the four integration constants for a given value of input intensity $I_{\text{in}} = |A_{\text{in}}|^2 = \varpi^{-2}|E_{\text{in}}|^2$. We then find the transmitted (output) intensity from the relation

$$I_{\text{tr}} = (1-\rho^2)I_+(L). \tag{8}$$

It is remarkable that, in spite of the complexity of the propagation equations, it is possible to solve them in an analytic form.

2.3. Optical bistability in the absence of thermo-optic effects

As discussed before, the preceding analytic solution is valid when the thermo-optic effect is negligible. In this case, we can find the bistable response function of the silicon resonator by inverting a transcendental relation $I_{\text{in}}(I_{\text{tr}})$, which can be expressed in an analytic form. As can be readily seen from Eq. (7a),

$$I_{\text{in}} = \frac{I_+(0) + \rho^2 I_-(0) - 2\rho\sqrt{C_1}\cos\Delta\phi}{1-\rho^2}, \tag{9}$$

where $\Delta\phi = 2\beta_0 L + \Delta\phi_{\text{NL}}$ and $\Delta\phi_{\text{NL}} = \phi_-(0) - \phi_+(0) - 2\beta_0 L$ is the nonlinear phase shift resulting from both the Kerr and free-carrier effects. From Eqs. (7b) and (8), we obtain

$$C_1 = I_+(L)I_-(L) = \frac{\rho^2}{(1-\rho^2)^2}I_{\text{tr}}^2. \tag{10}$$

Using this result and Eq. (7b) in Eq. (4), we can also express C_2 through I_{tr} as

$$C_2 = \coth^{-1}\left\{\frac{1}{a}\left[\frac{I_{\text{tr}}^2}{(1-\rho^2)^2} + b\right]\right\} - qL, \tag{11}$$

where a, b, and q are assumed to be functions of the transmitted intensity only. Finally, noting from Eq. (7b) that $\phi_+(L) = \phi_-(L) - 2\beta_0 L$, the nonlinear phase shift between the forward- and backward-propagating waves on the left facet of resonator is given by

$$\Delta\phi_{\text{NL}} = 3\gamma[\mathscr{J}_1(L) + \mathscr{J}_2(L) - \mathscr{J}_1(0) - \mathscr{J}_2(0)] - 2\xi_i[\mathscr{J}_3(L) - \mathscr{J}_3(0)]. \tag{12}$$

#118020 - $15.00 USD Received 1 Oct 2009; revised 6 Nov 2009; accepted 17 Nov 2009; published 18 Nov 2009

Substituting Eqs. (4) and (10)–(12) in Eq. (9), we obtain the input intensity $I_{\rm in}$ as a single-valued function of the transmitted intensity $I_{\rm tr}$. The multiple solutions of this equation for a given input intensity, $I_{\rm tr}(I_{\rm in})$, result from the phenomenon of optical bistability in SOI-waveguide-based resonators.

2.4. Inclusion of the thermo-optic effect

If no attempt is made to stabilize the resonator temperature, it increases because of heat generated through TPA and free-carrier recombination. In this case, the increase in resonator temperature $\Delta T(z)$ at point z results in a local change of the linear refractive index as

$$\Delta n_0(z) = \kappa \Delta T(z), \tag{13}$$

where $\kappa = 1.86 \times 10^{-4}$ K^{-1} is the thermo-optic coefficient of silicon. The temperature change in the region between z and $z+\Delta z$ can be found from a simple heat-balance equation,

$$\frac{\rho_m A_{\rm eff} \Delta z C \Delta T(z)}{\vartheta} = \beta \left[I_+^2(z) + I_-^2(z) + 4 I_+(z) I_-(z) \right] A_{\rm eff} \Delta z. \tag{14}$$

The right side of Eq. (14) gives the optical power absorbed through TPA that generates heat in the resonator volume $\Delta V = A_{\rm eff}\Delta z$. Its left side represents heat dissipation in the same volume, characterized by the thermal dissipation time ($\vartheta \sim 1$ μs), silicon mass density ($\rho_m = 2300$ kg/m^3), and silicon's thermal capacity [$C = 705$ J/(kg$\times$K)]. It is important to note that Eq. (14) accounts for temperature shift resulting from both TPA and recombination of free-carriers. This is because, owing to the initiation of these processes through phonon emission, the energy dissipated through TPA is fully converted to heat.

After obtaining $\Delta T(z)$ from Eq. (14) and using this result in Eq. (13), the nonlinear phase shift resulting from the thermo-optic effect is given by

$$\Delta \phi_{\rm NL}^{\rm T} = 2k \int_0^L \Delta n_0(z)\, {\rm d}z = 2k \frac{\kappa \vartheta \beta}{\rho_m C} \left[\mathscr{J}_3(L) - \mathscr{J}_3(0) \right], \tag{15}$$

where $\mathscr{J}_3(x)$ is given by Eq. (6c). Now, Eq. (9) can be extended to include a variable resonator temperature by setting $\Delta\phi = 2\beta_0 L + \Delta\phi_{\rm NL} + \Delta\phi_{\rm NL}^{\rm T}$.

It is interesting to note that the thermo-optic effect may be formally included by reducing the FCD coefficient, μ, by an amount

$$\Delta\mu = \frac{4\hbar\omega\kappa\theta k}{\rho_m C \sigma \tau}.$$

Using the parameter values mentioned earlier with $2\pi c/\omega = 1.55$ μm, and $\tau = 1$ ns [61], we obtain $\Delta\mu/\mu \approx 5.5$. Therefore, under typical operating conditions of a silicon-waveguide resonator, the thermo-optic effect dominates over the FCD effect. Obviously, the relative importance of FCD effect grows as the free-carrier lifetime is increased.

It is worthwhile to note that the energy dissipated through linear losses may also increase the resonator temperature and produce a nonlinear phase shift. By calculating the corresponding temperature shift using a heat-balance equation similar to that given in Eq. (14), it is easy to show that the linear-loss-induced change in the refractive index is equivalent to that resulting from the increase in the nonlinear Kerr parameter given by

$$\Delta n_2 = \frac{2\alpha\kappa\theta}{3\rho_m C}.$$

For a typical value of $\alpha = 1$ dB/cm, $\Delta n_2/n_2 \approx 300$, indicating that increase in the refractive index due to linear optical losses results in much higher nonlinear phase shift as compared to

#118020 - $15.00 USD Received 1 Oct 2009; revised 6 Nov 2009; accepted 17 Nov 2009; published 18 Nov 2009

that from the Kerr effect. Nevertheless, the phase shift due to linear losses is usually smaller than the phase shift given in Eq. (15) because TPA dominates over linear losses in the most of practical situations.

3. Discussion and numerical examples

3.1. Analytical investigation of the impact of FCA

In the absence of the TPA and free-carrier effects, the preceding analysis should reduce to the well-known equation describing optical bistability in fiber-based Fabry–Perot interferometers. To verify that this is indeed the case, we take the limits $\xi_r \to 0$ and $\xi_i \to 0$ in Eq. (9). Using Eqs. (4) and (11), we find that in this case $I_\pm$ are given by

$$I_+(z) = \frac{I_{\rm tr}}{1-\rho^2}\exp[-\alpha(z-L)], \quad I_-(z) = \frac{\rho^2 I_{\rm tr}}{1-\rho^2}\exp[\alpha(z-L)].$$

The functions in (6a) and (6b) are also simplified considerably in the above limits. As a result, Eq. (9) is reduced to the following relation between the input and transmitted intensities in lossy fiber resonators,

$$I_{\rm tr}\left(\frac{e^{\alpha L}-\rho^2 e^{-\alpha L}}{1-\rho^2}\right)^2\left\{1+\frac{4\rho^2}{(e^{\alpha L}-\rho^2 e^{-\alpha L})^2}\sin^2\left[\beta_0 L+\frac{3\gamma I_{\rm tr}L_{\rm eff}(\rho^2+e^{\alpha L})}{2(1-\rho^2)}\right]\right\} = I_{\rm in}, \quad (16)$$

where $L_{\rm eff} = [1-\exp(-\alpha L)]/\alpha$ is the effective length of the resonator. This expression reduces to the result in Ref. [71] if we neglect losses ($\alpha = 0$) and consider a high-finesse resonator.

To deduce the impact of FCA on optical bistability, we note from Eq. (4) that the presence of FCA leads to a gradual decrease in the forward-wave intensity and a corresponding saturation of output intensity with increasing input power. Indeed, $I_+(0) \to \infty$ as $C_2 \to 0$, which implies that an infinite input intensity is required in obtain a finite transmitted intensity [see Eqs. (9) and (11)]. It is easily deduced that the maximal transmitted intensity, $I_{\rm max}$ is determined from the transcendental equation

$$qL = \coth^{-1}\left\{\frac{1}{a}\left[\frac{I_{\rm max}^2}{(1-\rho^2)^2}+b\right]\right\}. \quad (17)$$

Since FCA dominates over the linear losses in the saturation regime, $\xi_r C_1 \gg \alpha$. Therefore, to a high degree of accuracy, Eq. (17) can be approximated by setting $q \approx 2\sqrt{3}\,\xi_r C_1$, $b \approx 2C_1$, and $a \approx \sqrt{3}C_1$. After these simplifications, Eq. (17) provides the following expression for the maximal output intensity:

$$I_{\rm max} \approx \left(\frac{1}{\rho}-\rho\right)\left[\frac{1}{2\sqrt{3}\,\xi_r L}\coth^{-1}\left(\frac{1+2\rho^2}{\sqrt{3}\,\rho^2}\right)\right]^{1/2}. \quad (18)$$

According to this expression, the maximal output intensity scales with the length of resonator and the free-carrier lifetime as $I_{\rm max} \propto (\tau L)^{-1/2}$. The fact that parameters L and τ enter Eq. (18) as a product is a direct consequence of cumulative nature of FCA. Obviously, FCD and the thermo-optic effect have no impact on the saturation process. The saturation of transmitted intensity induced by FCA reveals that optical bistability in silicon exhibits qualitatively distinct features compared with that in silica fibers [71–73].

An important conclusion that can be drawn from Eq. (18) is that $I_{\rm max}$ depends drastically on the mirror reflectivity ρ^2, approaching the maximum value $(2\xi_r L)^{-1/2}$ when $\rho \to 0$ and decreasing to zero when $\rho \to 1$. In practice, the coefficient ρ cannot be too small because optical

#118020 - $15.00 USD Received 1 Oct 2009; revised 6 Nov 2009; accepted 17 Nov 2009; published 18 Nov 2009

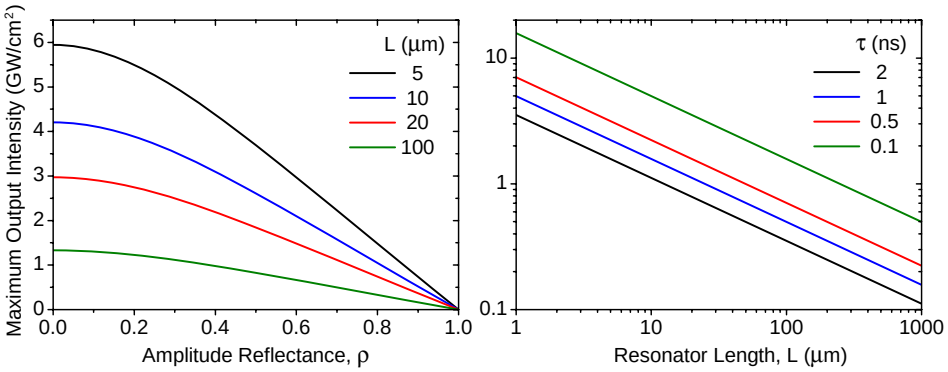

Fig. 2. Maximum output intensity in the FCA-induced saturation regime, $I_{\max}$, as a function of amplitude reflectance (left panel) and resonator length (right panel). In the left panel $\tau = 1$ ns, and $\rho = 0.7$ in the right panel.

bistability needs sufficient feedback. However, to observe optical bistability at reasonable input intensities, ρ should not be close to unity. This situation is in clear contrast to fiber resonators, where the facet reflectivities should be made as high as possible [71]. Ultimately, the optimum value of ρ is determined by the desirable input-output characteristic of the silicon resonator.

3.2. Numerical examples

The main features of the FCA-induced saturation of output power effect are illustrated by Fig. 2 where we show the dependance of maximum output intensity on amplitude reflectance and resonator length for an input optical beam at a wavelength of 1.55 μm. For this figure, we used the following typical parameter values for the silicon waveguide: $n_0 = 3.484$, $\beta = 0.5$ cm/GW, $n_2 = 6 \times 10^5$ cm^2/GW, and $\alpha = 1$ dB/cm. The facet reflectivities are assumed to be 70% in the right panel. As the figure indicates, the value of the maximum output intensity is approximately equal to 1.6 GW/cm^2 for a 10-μm resonator when $\tau = 1$ ns. This value is sufficiently large that optical bistability can be an useful tool even for a 10-μm-long silicon resonator.

We first illustrate the peculiarities of optical bistability in SOI-waveguide resonators in the absence of thermo-optic effects. The nonlinear phase shift in this case is given by Eq. (12). The impact of FCD, or free-carrier-induced changes in the refractive index, is included in this equation through the last term proportional to ξ_i. As this term is always negative, FCD reduces the nonlinear shift caused by the Kerr effect. Comparing the relative magnitudes of the free-carrier and Kerr terms in Eq. (12), we conclude that it is mainly the free-carrier effects, both FCA and FCD, that determine the input-output characteristics of silicon resonators at high input intensities.

The input-output characteristics of silicon resonators are shown in Fig. 3 for three resonators of different lengths. Longer resonators allow one to get more bistable regions within the same range of input intensities. In particular, resonator lengths of 20, 100, and 150 μm admit, respectively, 1, 4, and 5 bistable regions for input intensities below 5 GW/cm^2. This peculiarity simply reflects the fact that longer resonators accumulate more free carriers and produce larger phase shifts for a given input power than the shorter ones. Since the number of free carriers also grows with increasing I_{in}, the switching power successively increases as one goes from the first to second, third, *etc*. bistable regions. In contrast, switching power decreases for a given bistable region upon increasing the resonator length, but only at the expense of a reduced hysteresis width. For reference, red circles in Fig. 3(a) show the resonator transmittance calculated

#118020 - $15.00 USD Received 1 Oct 2009; revised 6 Nov 2009; accepted 17 Nov 2009; published 18 Nov 2009

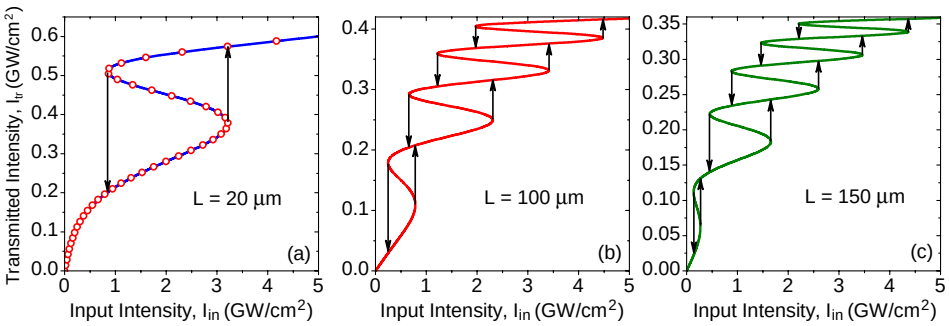

Fig. 3. Input-output characteristics of three silicon resonators in the absence of thermo-optic effects for $\rho = 0.7$ and $\tau = 1$ ns. Other parameters are the same as in Fig. 2. In the panel (a), red circles show the resonator transmittance calculated numerically in the presence of TPA. Portions of the curves with negative slopes represent unstable branches. Black arrows show abrupt changes occurring in I_{tr} at the boundaries of unstable regions.

numerically in the presence of TPA. This figure demonstrates an excellent agreement between the approximate analytical and the exact numerical results. In the case where the contribution of TPA cannot be ignored, numerical simulations do not reveal any qualitative difference between the true bistable response of silicon resonator and that predicted by Eq. (9). Therefore, all the findings based on our approximate analysis remain valid in the presence of TPA, and thus can be considered justified under general conditions.

It is interesting to note that the effects of optical bistability may be observed even in an ordinary SOI waveguide without reflecting coatings at its ends. This scenario is illustrated by the left panel in Fig. 4, where transmitted intensity is plotted as a function of input intensity for three 20-μm-long resonators with different facet reflectivities. The red curve in this panel, corresponding to the natural reflectance of the silicon/air interface ($\rho = 0.5$), clearly exhibits a bistable character. The results, presented in the left panel of Fig. 4, reveal the disadvantages associated with the use of highly-reflectivity mirrors, the most notable being a substantial increase required in the input intensity for optical switching with increasing ρ. The crucial role of FCD in the formation of optical bistability in silicon is illustrated in the right panel of Fig. 4. The

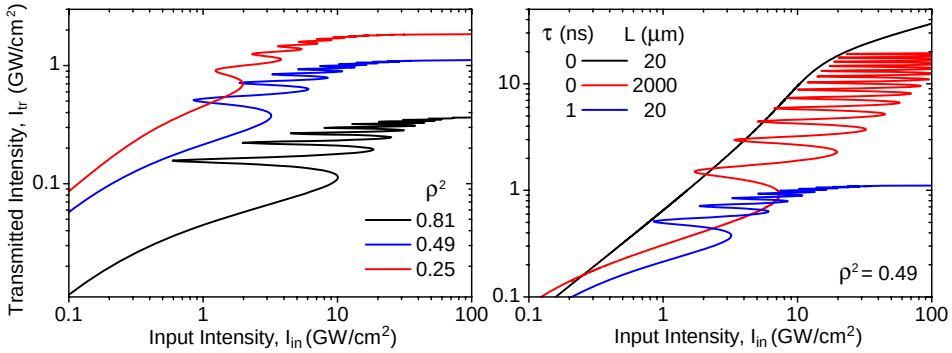

Fig. 4. The impact of mirror reflectivities (left) and free-carrier lifetime (right) on the bistable characteristics of silicon resonators. In the left panel, $\tau = 1$ ns and $L = 20$ μm. In the right panel, $\tau = 0$ curves show device behavior in the absence of free-carrier effects. For simulation parameters, see the text.

#118020 - $15.00 USD Received 1 Oct 2009; revised 6 Nov 2009; accepted 17 Nov 2009; published 18 Nov 2009

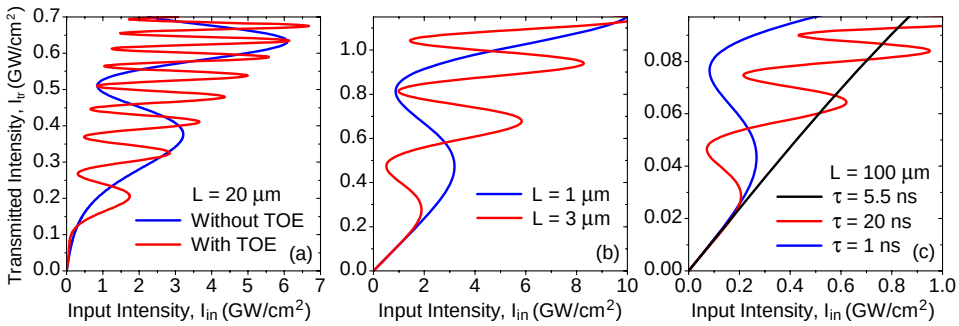

Fig. 5. Impact of thermo-optic effects on optical bistability in silicon resonators with $\rho = 0.7$. (a) Bistability curves for a 20-μm-long resonator with (red) and without (blue) thermo-optic effects for $\tau = 1$ ns; (b) bistable behavior for two ultrashort resonators with $\tau = 1$ ns; (c) input-output characteristics of a 100-μm-long resonator for three values of τ.

blue and black curves in this panel characterize the transmittance of a 20-μm-long resonator with and without free-carriers, respectively. One can see that, in the absence of FCD, optical bistability is unattainable for input intensities below 100 GW/cm^2. The red curve for $L = 2$ mm shows that purely Kerr-induced bistability can occur for much longer resonators. From a practical standpoint, free-carrier effects cannot be made negligible. In fact, their presence is beneficial because optical bistability can be realized in much shorter resonators.

We now consider the role of thermo-optic effects excluding increase in the refractive index resulting from heat generation due to linear losses. Figure 5(a) shows the comparison between bistable characteristic of a 20-μm-long silicon resonator with and without the thermo-optic effect. According to our theory, the presence of thermo-optic effect introduces an additional nonlinear phase shift [see Eq. (15)] that affects the bistable behavior in a quantitative fashion. More specifically, the presence of thermo-optic effects reduces input intensities at which bistable switching occurs and increases the number of bistable regimes. Moreover, optical bistability may occur even for much shorter resonators in the presence of thermo-optic effects. Figure 5(b) shows that bistability can occur even in a 1-μm-long silicon resonator at input intensities ~ 1 GW/cm^2. As shown in Fig. 5(c), required intensities can be reduced to levels below 0.3 GW/cm^2 by using a 100-μm-long silicon resonator. Notice that long carrier lifetimes are actually beneficial for observing optical bistability [see the red curve in Fig. 5(c)]. However, when the compensation between FCD and thermo-optic effects occurs in short resonators, the bistability phenomenon disappears [see the black line in Fig. 5(c)].

The dependance of bistable characteristics of silicon resonators on the effective free-carrier lifetime, resonator length, and facet reflectivities allows one to engineer their optical response according to practical needs. Our results show that optical bistability and multistability can occur in ultrashort SOI waveguides even without facet coatings and suggest that nanoscale silicon resonators are promising devices for optical switching.

3.3. Optical switching at a fixed bias intensity

The dependance of resonator transmittance on the effective free-carrier lifetime τ can be exploited to realize optical switching in silicon resonators electronically at a fixed input intensity. The reason is that the number of free electrons and holes inside a silicon resonator can be controlled by applying an external voltage across a reverse-biased p-n junction. The dc electric field induced by this voltage removes free carriers from the region where light is concentrated. Such a change in the free-carrier density can lead to an effective reduction in τ, which can be

#118020 - $15.00 USD Received 1 Oct 2009; revised 6 Nov 2009; accepted 17 Nov 2009; published 18 Nov 2009

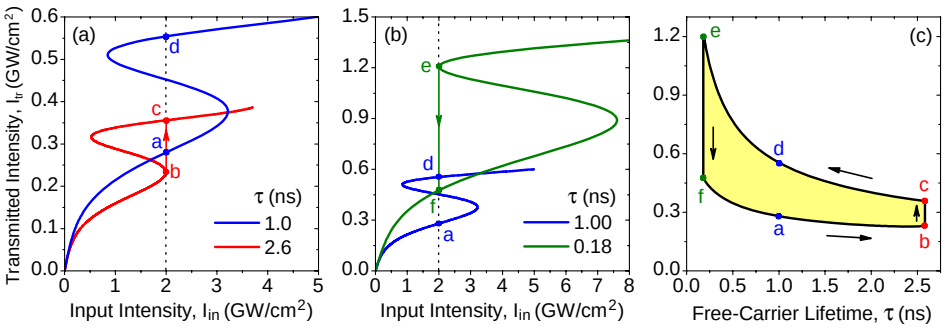

Fig. 6. Demonstration of optical switching in a silicon resonator by varying τ though an external voltage. Panels (a) and (b) show changes in the bistable characteristics of a silicon resonator as τ changes from $1 \to 2.6 \to 1$ ns and $1 \to 0.18 \to 1$ ns, respectively. Panel (c) shows hysteresis loop in the $I_{\rm tr}$-τ domain. The input intensity is fixed at 2 GW/cm^2 with $\rho = 0.7$ and $L = 20$ μm.

considered as a controllable parameter.

The process of optical switching induced by varying the free-carrier lifetime is illustrated in Fig. 6. The first two panels of this figure show input-output characteristics of a 20-μm-long resonator for different values of τ (without thermo-optic effects). To demonstrate the switching up of the resonator output, suppose that initially $\tau = 1$ ns [blue curve in Fig. 6(a)]. Then, if the input (bias) intensity is kept fixed at $I_b = 2$ GW/cm^2, the system is in the state a with $I_{\rm tr,a} \approx 0.28$ GW/cm^2. If we now gradually increase τ, the blue curve in Fig. 6(a) shrinks due the growth of FCD contribution until it coincides with the red curve at $\tau = 2.6$ ns. At the same time, the output intensity decreases to $I_{\rm tr,b} \approx 0.23$ GW/cm^2 as the system comes to state b. As τ is increased still further, the system jumps to state c characterized by $I_{\rm tr,c} \approx 0.36$ GW/cm^2. If now we reduce the free-carrier lifetime back to 1 ns, the red curve will transform back to the blue curve, and the system turns to state d with $I_{\rm tr,d} \approx 0.55$ GW/cm^2. Hence, by changing the free-carrier lifetime from $1 \to 2.6 \to 1$ ns, we transferred the system from state a to state d and changed the output intensity from 0.28 to 0.55 GW/cm^2.

The inverse process of switching the system down from state d to state a is illustrated in Fig. 6(b). As one decreases the free-carrier lifetime from 1 to 0.18 ns, the blue curve in this figure stretches and takes the shape of the green curve. As a result, if the bias intensity is kept fixed at 2 GW/cm^2, the system jumps from state d to state e with $I_{\rm tr,e} \approx 1.2$ GW/cm^2. If we continue to decrease τ further, the system jumps to state f, and the transmitted intensity reduces to $I_{\rm tr,f} \approx 0.48$ GW/cm^2. Finally, increasing the free-carrier lifetime back to 1 ns, we force the resonator to arrive at the initial state a.

The preceding scheme of optical switching is represented by the hysteresis loop shown in Fig. 6(c). As seen clearly on this figure, one can switch the system between the states a and d by varying τ and moving counterclockwise along the hysteresis loop (the clockwise bypass is not possible because the segments b-c and e-f are irreversible). In this case, the intensity jump is given by $\Delta I_{\rm tr} = I_{\rm tr,d} - I_{\rm tr,a} \approx 0.27$ GW/cm^2 when the resonator is biased with $I_b = 2$ GW/cm^2. It is possible to vary the value of $\Delta I_{\rm tr}$ from 0 to $\Delta I_{\rm max} = I_{\rm tr,e} - I_{\rm tr,b} \approx 0.97$ GW/cm^2.

As a concluding remark, we would like to emphasize that the condition $\alpha\xi_r \gg \beta^2$, guaranteeing the validity of the presented analytical solution, is a very strong condition and in some situations may be softened. Once the inequality $\alpha\xi_r \gg \beta^2$ is satisfied, TPA is dominated by either linear losses or FCA in the whole range of input powers and, therefore, can be safely neglected. However, if it is not satisfied, this does not imply that inclusion of TPA will necessarily

#118020 - $15.00 USD Received 1 Oct 2009; revised 6 Nov 2009; accepted 17 Nov 2009; published 18 Nov 2009

change the resonator response since, in the range of intensities where TPA exceeds other dissipation sources, all of them may be negligible. This is indeed happens when the above inequality fails to hold for high-finesse silicon resonators with linear optical losses below 0.1 dB/cm.

4. Conclusions

In this paper, we have developed a theoretical model that describes accurately the nonlinear phenomenon of optical bistability in Fabry–Perot types silicon-waveguide resonators. To make the analysis as general as possible, we have include three sources of the nonlinear phase shift, namely the Kerr effect, free-carrier-induced index shift (FCD), and the thermo-optic effect. In addition, our model includes three sources of losses, namely the linear scattering loss, TPA, and FCA. Even though our model involves both the forward- and backward-propagating modes inside the resonator, we were able to solve analytically the set of four nonlinear equations for the mode intensities and phases in the case of a continuous-wave (CW) input field. Using this analytical solution together with the boundary conditions at the resonator facets, we were able to obtain a transcendental equation relating the output intensity to the input intensity. Even though our analysis is done for CW fields, the results may be applicable to optical pulses as well as long as pulses are not so short that group-velocity dispersion begins to play an important role.

Our analysis reveals a dual role of free carriers in the formation of optical bistability in silicon. First, FCA results in saturation of the transmitted intensity. Second, the FCD and the thermo-optic effect introduce phase shifts far exceeding those resulting from the Kerr effect alone. We show that free carriers, while reducing output intensities because of FCA, also enable one to achieve optical bistability in ultrashort resonators that are only a few micrometers long. Moreover, bistability can occur even when waveguide facets are not coated because natural reflectivity of the silicon/air interface can provide sufficient feedback. In fact, high-reflectivity coatings generally degrade the bistable response of silicon-waveguide resonators because FCA effects become much more dominant in high-Q resonators.

In addition to conventional bistable switching realized by changing input power levels, we show that a new type of electronic switching is possible in silicon-waveguide resonators. Since both the FCA and FCD depend on the accumulation of free carriers, it is possible to realize optical switching by changing the free-carrier lifetime electronically (e.g., using a reverse-biased p-n junction). Such an electronically assisted optical switching at a fixed input power may prove beneficial for a multitude of applications and may lead to silicon-based, nanometer-size, optical memories.

Acknowledgment

This work was funded by the Australian Research Council through its Discovery Grant scheme under grant DP0877232. The work of GPA is also supported by the NSF award ECCS-0801772.

#118020 - $15.00 USD Received 1 Oct 2009; revised 6 Nov 2009; accepted 17 Nov 2009; published 18 Nov 2009